

# Expression of the Type 1 Insulin-like Growth Factor Receptor Is Up-Regulated in Primary Prostate Cancer and Commonly Persists in Metastatic Disease<sup>1</sup>

Giles O. Hellawell, Gareth D. H. Turner, David R. Davies, Richard Poulson, Simon F. Brewster, and Valentine M. Macaulay<sup>2</sup>

Molecular Oncology Laboratories, Weatherall Institute of Molecular Medicine, Oxford OX3 9DS [G. O. H., V. M. M.]; Department of Cellular Pathology, John Radcliffe Hospital, Oxford OX3 9DU [G. D. H. T., D. R. D.]; Histopathology Unit, Cancer Research UK Laboratories, Lincoln's Inn Fields, London WC2A 3PX [R. P.]; and Department of Urology, Churchill Hospital, Oxford OX3 7LJ [G. O. H., S. F. B.], United Kingdom

## ABSTRACT

The type 1 insulin-like growth factor receptor (IGF1R) mediates tumor cell growth, adhesion, and protection from apoptosis. High plasma IGF-I levels predispose to prostate cancer, but there is no consensus regarding IGF1R expression in primary and metastatic prostate cancer. Recent studies in a human cell line and a mouse model suggest that metastatic prostate cancer cell detachment may be favored by impairing cadherin function via loss of expression of insulin receptor substrate-1 (IRS-1), the principal IGF1R docking molecule. This may be accompanied by PTEN mutation, reactivating a key antiapoptotic pathway, and by IGF1R down-regulation to prevent Shc-mediated differentiation. We studied IGF1R expression in 54 samples of primary prostate tissue including 44 archival and 10 prospectively collected biopsies. We performed semiquantitative immunostaining for the IGF1R, IRS-1, and PTEN, and *in situ* hybridization for IGF1R. The IGF1R was significantly up-regulated at the protein and mRNA level in primary prostate cancer compared with benign prostatic epithelium. There was a trend toward increased expression of IRS-1 in the malignant biopsies. We also measured IGF1R, IRS-1, and PTEN expression in 12 paired biopsies of primary prostate cancer and subsequent bone metastases. In four cases, IGF1R and IRS-1 levels were lower in the metastases than in the primary tumors. Three of these metastases also lacked significant PTEN staining, compatible with findings in the model systems described above. However, this pattern was relatively uncommon, and 8 of 12 cases expressed detectable IGF1R and IRS-1 in both primary and metastatic biopsies. These findings challenge earlier reports of IGF1R down-regulation in metastatic disease and reinforce the importance of the IGF1R in prostate cancer biology.

## INTRODUCTION

Prostate cancer is the commonest cancer in men, and the second commonest cause of male cancer deaths in the United States and the United Kingdom (1, 2). Metastatic prostate cancer most commonly affects the bones and is initially androgen dependent. However the development of androgen independence is inevitable, usually after 12–18 months of endocrine therapy (3). Prostate cancer is essentially chemoresistant, and there is an urgent need for new treatments to improve the outlook for patients with advanced androgen-independent disease.

The IGFs<sup>3</sup> -I and -II and the IGF1R play a critical role in the establishment and maintenance of the transformed phenotype. Overexpression of the IGF1R induces growth, neoplastic transformation, and tumorigenesis (4). IGFs induce tumor cell motility via cross-talk between the IGF axis and the integrin system (5, 6). Work by us and

others has shown that the IGF1R and its principal docking molecule IRS-1 can influence cell-cell interactions by modulating interaction between components of adherens junctions (7–9). Compared with equivalent normal tissues, the IGF1R is overexpressed by tumors including colorectal cancer and melanoma (10–12), and IGF1R overexpression has been linked to radioresistance in breast cancer (13). In mouse melanoma cells, we showed that antisense-mediated IGF1R down-regulation is associated with enhanced sensitivity to ionizing radiation, and with impaired activation of Atm, the product of the gene mutated in ataxia telangiectasia (14). This suggests an important role for the IGF system in the cellular response to DNA damage and supports the concept of IGF1R targeting as novel therapy for radio- and chemoresistant cancers that overexpress this receptor.

The IGF axis appears to contribute to prostate cancer pathogenesis. Elevated levels of plasma IGF-I and reduced levels of the main serum-binding protein, IGF-BP3, are associated with an increased risk of prostate cancer (15, 16). The IGFs and the IGF1R are detectable in human prostate stroma and epithelial cells (17, 18). There is, however, no consensus regarding relative levels of IGF1R expression in benign and malignant prostate epithelium and the role of the IGF1R in metastasis. Tennant *et al.* (18) reported that IGF1R expression is significantly lower at the protein and RNA level in malignant *versus* benign prostatic epithelium. Several studies found no difference in IGF1R levels, measured by immunostaining and immunoblotting, between benign and malignant prostate tissue (19, 20). Furthermore, IGF1R expression is reportedly absent in bone metastases in patients with androgen-independent prostate cancer (19).

Prostate-specific expression of SV40 large T antigen has been shown to lead to the development of prostate adenocarcinomas in transgenic mice. The tumors metastasize predominantly to lymph nodes and lung rather than to bone (21). In this TRAMP model, IGF1R levels are unchanged during the development of primary prostate cancers and are dramatically down-regulated in metastatic lesions (22). A possible explanation for this finding has been proposed after studies in the human prostate cancer cell line, LNCaP, which originated from a metastatic tumor (23, 24). LNCaP cells lack IRS-1 because of promoter methylation and have relatively low IGF1R levels (9, 25). Loss of IRS-1 could enhance the propensity for metastasis by impairing the function of integrins and E-cadherin, thus favoring metastatic cell detachment (9). Both IRS-1 and Shc bind to Tyr 950 in the IGF1R juxtamembrane domain (26). In the absence of IRS-1, the predominant action of the IGF1R may be to induce terminal differentiation via the Shc/mitogen-activated protein kinase pathway. This scenario could be avoided by IGF1R down-regulation (24). LNCaP cells also have a frameshift mutation in *PTEN*. This is a tumor suppressor gene encoding a phosphatase that antagonizes the action of phosphatidylinositol 3'-kinase (27). In human prostate cancer tissue, the loss of PTEN expression is correlated with Gleason score and advanced pathological stage (28). Loss of functional PTEN protein ensures that in the absence of IRS-1 there is constitutive activation of the Akt pathway for apoptosis protection (29).

To clarify the role of the IGF1R in prostate cancer, we have

Received 12/14/01; accepted 3/18/02.

The costs of publication of this article were defrayed in part by the payment of page charges. This article must therefore be hereby marked *advertisement* in accordance with 18 U.S.C. Section 1734 solely to indicate this fact.

<sup>1</sup> Supported by the PPP Foundation and by Cancer Research UK.

<sup>2</sup> To whom requests for reprints should be addressed, at IGF Group, Molecular Oncology Laboratories, Weatherall Institute of Molecular Medicine, John Radcliffe Hospital, Oxford OX3 9DS UK. Phone: 44(0)1865-222433; Fax: 44(0)1865-222431; E-mail: macaulay@cancer.org.uk.

<sup>3</sup> The abbreviations used are: IGF, insulin-like growth factor; BPH, benign prostatic hyperplasia; IGF1R, type 1 IGF receptor; IGF BP, IGF binding protein; IRS-1, insulin receptor substrate-1; PSA, prostate-specific antigen; TRAMP, transgenic adenocarcinoma of mouse prostate; TURP, transurethral resection of the prostate.

undertaken a study of IGF1R expression at the protein and mRNA level in biopsies of primary and metastatic prostate cancer. To assess the functional significance of IGF1R expression, we have also analyzed expression of IRS-1 and PTEN. We found clear evidence of IGF1R up-regulation in primary prostate cancers compared with benign prostate epithelium. We also analyzed paired biopsies obtained from 12 patients who underwent a diagnostic biopsy of a primary prostate adenocarcinoma, and subsequently developed androgen-independent metastatic disease. Three cases showed significant reduction/loss of IGF1R, IRS-1, and PTEN expression compatible with the findings in prostate cancer model systems. However the majority of cases that we studied retained IGF1R and IRS-1 expression. This suggests that the model systems described above have only limited relevance to clinical disease, and that IGF1R down-regulation and IRS-1 loss are not prerequisites for prostate cancer metastasis.

## MATERIALS AND METHODS

**Tissue Samples.** Formalin-fixed, paraffin-embedded fine-needle biopsy specimens were collected retrospectively from archival material stored in the Department of Pathology at the John Radcliffe Hospital, Oxford, United Kingdom. All of the biopsies had been taken during a recent 6-month period (January to July, 1999). Twenty-two benign biopsies had been obtained from patients with median age 67 years (range, 49–80 years). All of the patients had lower urinary tract symptoms and a benign prostate on digital rectal examination, and all had been referred for biopsy on account of an elevated PSA [median, 11.5 ng/ml; range, 3.1–18 ng/ml (normal range 0–4)]. None of these patients have subsequently developed prostate cancer. Twenty-two malignant biopsies were obtained from prostate cancer patients with median age 74 (range, 54–78 years). All had localized (stage T<sub>1c</sub>) tumors, and the median PSA for this group was 16.1 ng/ml (range, 7.7–200 ng/ml). The median total Gleason score for the malignant biopsies was 7 (range, 5–9) with a median Gleason grade of 3 in the individual areas stained for IGF1R and IRS-1. All of the biopsies had been fixed immediately in 10% buffered formalin, and 24 h later, had been dehydrated in ascending concentrations of alcohol and embedded in paraffin. Adjacent 5- $\mu$ m sections from the paraffin blocks were stained with H&E and served as a histopathological guide during evaluation of immunohistochemistry.

Fresh prostate biopsy samples were obtained prospectively with informed consent from 10 patients undergoing TURP at the Churchill Hospital, Oxford, United Kingdom. Five patients had BPH (median age, 76; range, 57–85 years), with no indication of prostate malignancy on digital rectal examination or transrectal ultrasound, and serum PSA values of  $\leq$ 0.1 ng/ml. Biopsies were also obtained from five patients with malignant disease (median age, 64 years; range, 56–79 years; median PSA, 100 ng/ml; range, 66–1700 ng/ml) attending for a “channel” TURP after progression of known adenocarcinoma. The cancers had a median total Gleason score of 8 (range, 6–9), and the stained sections had a median grade of 4 in the areas used for immunostaining. At the time of surgery, one patient had been on antiandrogen therapy for 2 days, with no overt histopathological sequelae, and none of the other patients had any previous endocrine therapy. A single resection chip was bisected, and one-half was placed in 10% buffered formalin for 24 h, and processed to paraffin. Sections were H&E stained to assess tissue pathology, and adjacent sections were used for *in situ* hybridization. The other half was snap-frozen in liquid nitrogen for protein analysis.

We obtained archival paraffin-embedded samples of metastatic prostate cancer from the Nuffield Orthopaedic Centre, Oxford. These were from patients who had undergone hip replacement surgery after pathological fracture through a deposit of metastatic adenocarcinoma. Of 38 patients identified, there were 25 cases in which the metastatic tumor stained positive for PSA and prostatic acid phosphatase. These cases were further limited to those from whom an initial, diagnostic prostate cancer biopsy was available from the John Radcliffe Hospital, leaving a total of 12 paired tumor samples. At the time of the diagnostic prostate biopsy, the 12 patients had a median age of 70 years (range, 57–84). The median total Gleason score for the initial biopsy was 8 (range, 5–9), and all of the tumors were stage  $\leq$ T<sub>3</sub>. No patients were receiving endocrine therapy at that time, but all subsequently received antiandrogens for

metastatic disease. At the time of pathological fracture, all 12 patients had progressive disease that was clinically and biochemically (PSA) androgen-independent, with a median PSA of 184 ng/ml (range, 77–402 ng/ml).

**Cell Lines.** Human prostate cancer cell lines DU145 and PC3 (androgen-independent) were obtained from the Cancer Research UK Laboratories, Clare Hall, South Mimms, United Kingdom, and the LNCaP cell line (androgen-dependent) was a gift of Dr. Renato Baserga. All of the cell lines have been reported to express the IGF1R, and LNCaP cells fail to express IRS-1 (9, 30–32). The DU145 and LNCaP cell lines were cultured in RPMI 1640 plus 10% FCS. PC3 cells were cultured in Ham's F12 with 10% FCS. Cell lines R<sup>-</sup> and R<sup>+</sup> were also from Dr. Baserga. R<sup>-</sup> cells are 3T3-like cells derived from IGF1R knockout mice, and R<sup>+</sup> cells are R<sup>-</sup> cells that overexpress the human IGF1R (33). These cells were cultured in DMEM plus 10% FCS. All of the cultures were maintained in a humidified atmosphere of 5% CO<sub>2</sub>, and all were negative for *Mycoplasma* infection. To prepare cell pellets, monolayers were disaggregated using 3 mM EDTA in PBS. The cells were pelleted at 1200 rpm for 5 min, and the pellet was fixed overnight in neutral buffered formalin. Pellets were embedded in paraffin and 5- $\mu$ m sections were used as controls for the specificity of immunohistochemical staining.

**Immunohistochemistry.** All of the cell pellet and tissue sections were freshly cut to minimize decay in tissue immunoreactivity (34). The 5- $\mu$ m sections were dewaxed, rehydrated through graded ethanol washes, and immersed in PBS. Slides were incubated with 0.3% hydrogen peroxide for 5 min, washed with PBS, and blocked in PBS plus 10% normal swine serum for 15 min. Excess blocking buffer was removed, and IGF1R staining was performed with a polyclonal antibody to the IGF1R  $\beta$  subunit (Santa Cruz Biotechnology, Santa Cruz, CA), using a modification of a previously described method (13). The antibody was used at a dilution of 1:750, and slides were incubated overnight at 4°C in a humidified chamber. After washing, bound antibody was detected using a polymer-labeled enhancement system (DAKO Envision+ System, Peroxidase (DAB); DAKO Corporation, Carpinteria, CA). Slides were incubated for 30 min with a peroxidase-labeled polymer conjugated to goat antirabbit immunoglobulins. Immune complexes were visualized with the chromogenic substrate diaminobenzidine, and slides were counterstained with hematoxylin and mounted. Control sections were stained with the IGF1R $\beta$  antibody preabsorbed with a 5-fold molar excess of the peptide to which the antibody had been raised. IRS-1 staining was performed using a polyclonal IRS-1 antibody (A19; Santa Cruz Biotechnology), used at a 1:100 dilution, and slides were incubated for 30 min at room temperature. Bound antibody was detected as above using the DAKO Envision+ System, and slides were counterstained with hematoxylin and mounted. Sections of LNCaP and DU145 cell pellets were used as negative and positive controls respectively, for IRS-1 staining.

PTEN immunohistochemistry used a modification of a previously published technique (28, 35). Slides were immersed in 10 mM citrate buffer (pH 6), and antigen retrieval was conducted in a pressure cooker for 5 min. The slides were cooled at room temperature in PBS, and endogenous peroxidase activity was blocked by incubating in 0.3% hydrogen peroxide for 5 min. After blocking in 10% swine serum in PBS, slides were incubated with 1:1500 dilution of polyclonal PTEN antibody (Upstate Biotech, Lake Placid, NY) overnight in a humidified chamber. After washing, bound antibody was detected using the DAKO Envision+ System as described above. DU145 and PC3 cells were used as positive and negative controls, respectively.

Preliminary staining of cell pellets (not shown) established the optimal antibody dilution for each analysis. The final dilution selected was that which resulted in clear positive staining for IGF1R in R<sup>+</sup> cells, and for IRS-1 and PTEN in DU145, without detectable staining in the negative control sections made, respectively, from R<sup>-</sup>, LNCaP, and PC3 cells. These antibody dilutions were used for staining of tissue sections. To avoid interassay variability, all of the sections used for quantitation were from the same staining run. Scoring was conducted independently by two observers (G. O. H. and D. R. D.) who were blinded to the clinical diagnosis of the patient and, in the case of the malignant specimens, to the overall Gleason score. As described previously (13), IGF1R staining intensity was rated on a 4-point scale: 1+, none or minimal; 2+, light; 3+, moderate; 4+, heavy. For quality control purposes, each staining run included a section of primary prostate cancer that was scored as 3+. In addition to scoring intensity, the distribution of staining was recorded as focal or diffuse, and membranous or cytoplasmic. The same 4-point scale was used for semiquantitative analysis of immunostaining for IRS-1. PTEN staining of

malignant epithelia was generally of uniform intensity, although there were significant differences in the extent of positivity. This was scored as 0, no staining; 1+, mixed areas of positivity and negativity; 2+, all tumor cells positive, as described previously (28). Data analysis used SPSS software (SPSS Inc., Chicago, IL), and differences between groups were compared by the Mann-Whitney test.

**In Situ Hybridization.** *In situ* hybridization was performed on formalin-fixed paraffin sections of prospectively collected benign and malignant prostate chips, using riboprobes labeled internally with  $^{35}\text{S}$  (~800 Ci/mmol; Amersham Pharmacia; Ref. 36). To detect IGF1R mRNA, a 2.2-kb *SphI* fragment of human IGF1R cDNA (a gift of Dr. Baserga) representing bases 952-3164 of the sequence (37) was cloned into *SphI*-digested pGEM-5Zf(+) vector (Promega). Clone IGF1R-*SphI*-AS was linearized with *SmaI* to make a DNA template that generated a 428-base antisense probe (bases 3164-2736 of the IGF1R transcript) on *in vitro* transcription with T7 RNA polymerase. Clone IGF1R-*SphI*-S, incorporating the IGF1R insert in a sense orientation with respect to the T7 promoter, was used to make a control sense template by digesting with *AatII* and *SmaI*, blunting with Klenow enzyme, and religating to excise unwanted sequence from bases 952-2736. This construct, linearized with *MluNI*, generated a 398-base sense riboprobe with T7 RNA polymerase, representing bases 2736-3134 of the IGF1R transcript. A  $\beta$ -actin probe of ~450 bases was used as a control for the presence of intact hybridizable mRNA (38).

## RESULTS

**The IGF1R Is Overexpressed by Malignant Human Prostatic Epithelium.** To validate the specificity of immunocytochemical staining for IGF1R, preliminary analyses were performed on R+ and R- cell pellets. Using the IGF1R $\beta$  antibody at 1:750 dilution and without antigen retrieval, we saw no staining in the R- cells, which lack IGF1R. We noted that false-positive staining was detectable in

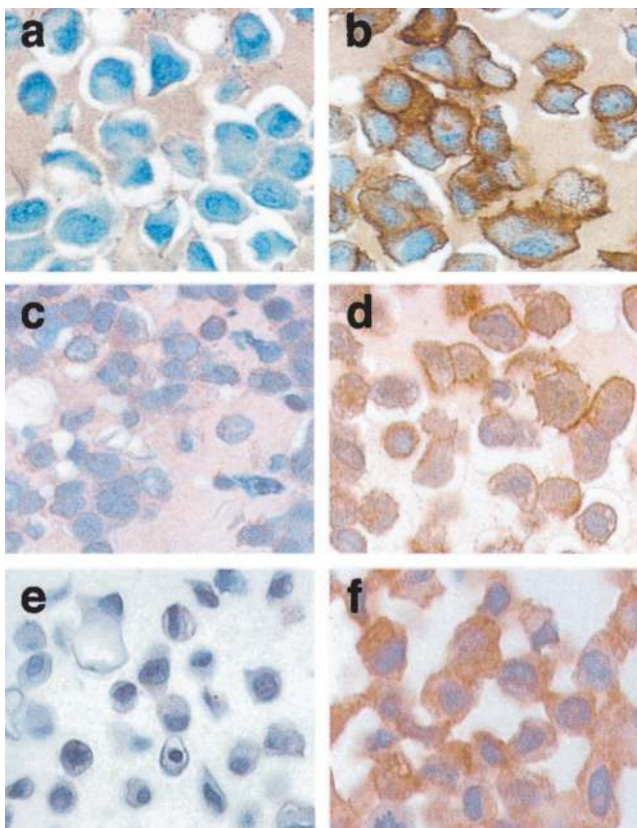


Fig. 1. Use of formalin-fixed cell pellets to validate the specificity of immunostaining for IGF1R, IRS-1, and PTEN. *a*, R- cells stained for IGF1R; *b*, R+ cells stained for IGF1R; *c*, LNCaP cells stained for IRS-1; *d*, DU145 cells stained for IRS-1; *e*, PC3 cells stained for PTEN; *f*, DU145 cells stained for PTEN.  $\times 400$ .

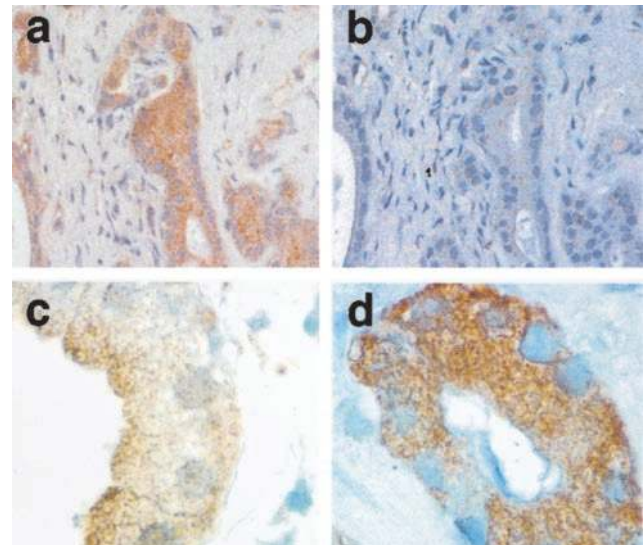


Fig. 2. Specificity and distribution of IGF1R immunostaining in fine-needle biopsies of prostate. *a*, section of prostate cancer showing diffuse brown staining predominantly in the epithelium, with lighter staining in the less cellular stroma ( $\times 200$ ). *b*, adjacent section showing no significant staining using IGF1R $\beta$  antibody after preincubation with 5-fold molar excess of peptide to which the antibody was raised ( $\times 200$ ). *c*, section of benign biopsy showing accentuation of IGF1R staining at the luminal surface of the epithelium ( $\times 400$ ). *d*, section of malignant epithelium showing diffuse intracellular staining for IGF1R ( $\times 400$ ).

R- cells after the use of antigen-retrieval techniques (*e.g.*, microwaving) or higher concentration of anti-IGF1R $\beta$  antibody. Indeed, antigen retrieval for the IGF1R has been shown to be unnecessary in previous studies (10, 18). All of the subsequent immunostaining was performed without antigen retrieval and with 1:750 dilution of primary antibody. In the R+ cells, which express  $\sim 10^6$  human IGF1R/cell (33), clear peripheral staining was observed (Fig. 1, *a* and *b*), reflecting the location of the IGF1R at the cell membrane. Tissue fixation reportedly disrupts the cell membrane in paraffin-embedded specimens, leading to membranous and cytoplasmic staining as shown previously (13, 18). During our initial optimization of IGF1R immunostaining on tissue samples, we found that sections of radical prostatectomy blocks and TURP chips gave inconsistent results because of variable tissue fixation (not shown). In contrast, staining of small caliber (1-2 mm) fine-needle biopsies provided consistent results, reflecting uniform fixation and tissue preservation.

IGF1R immunostaining was predominantly localized to the glandular epithelium (Fig. 2*a*), with lower levels in the stroma and more intense staining in neurovascular bundles (not shown). No significant staining was seen when the IGF1R antibody was preabsorbed with the IGF1R peptide to which it had been raised (Fig. 2, *a* and *b*). There was a difference in the distribution of IGF1R immunoreactivity at the tissue and cellular levels. Within individual epithelial cells, the staining was predominantly on the luminal aspect of benign cells and was more diffuse in the malignant epithelial cells (Fig. 2, *c* and *d*). At the tissue level, IGF1R staining was predominantly focal in benign epithelium, and diffuse (*i.e.*, involving most/all areas of epithelium) in the malignant biopsies (Figs. 3 and 4). Fig. 3 shows representative examples of immunostained fine-needle biopsy sections from benign prostate that were scored as 1+ (Fig. 3*a*) and 2+ (Fig. 3*b*) and from malignant prostate that were scored as 3+ (Fig. 3*c*) and 4+ (Fig. 3*d*). The results of analysis of all 44 cases are shown in Fig. 4. Of the 22 benign biopsies, 17 (77%) showed negligible (1+) or light (2+) staining for IGF1R. In contrast 21 (95%) of the 22 samples of malignant prostatic epithelium showed moderate (3+) or heavy (4+) staining. This indicates significant overexpression of the IGF1R in malignant versus benign prostatic epithelium ( $P < 0.05$ ).

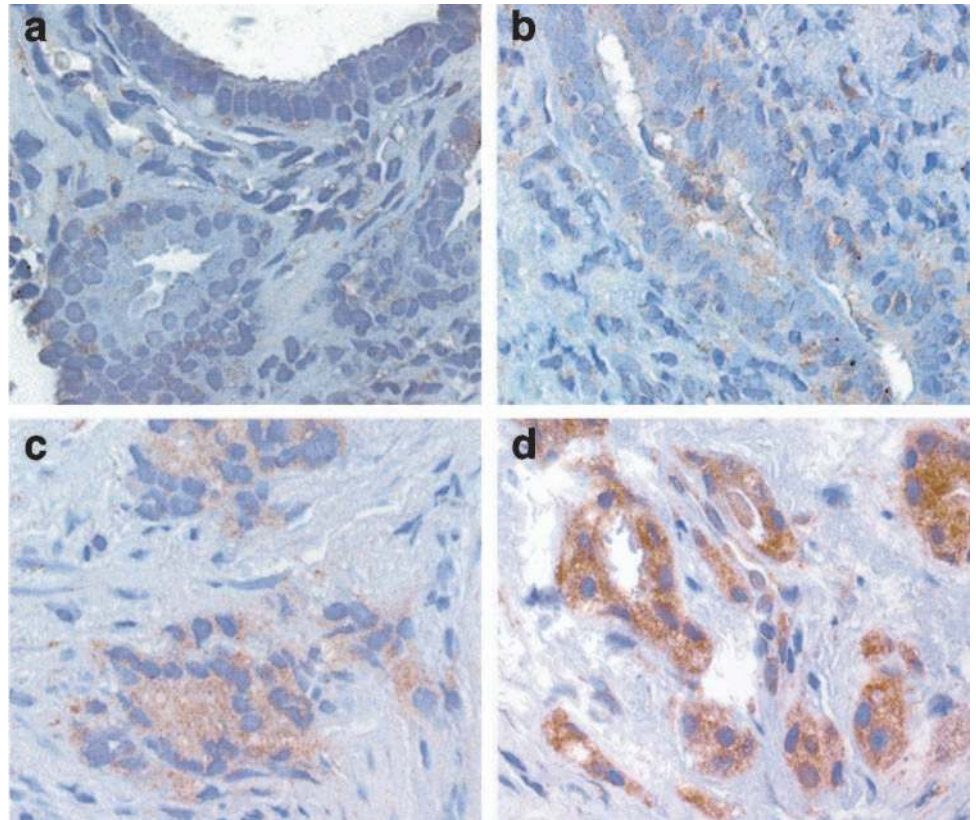


Fig. 3. Immunohistochemical staining of IGF1R expression in fine-needle biopsies of prostate. Representative sections are shown ( $\times 400$ ) to illustrate staining that was scored as *a*, 1+ (benign biopsy); *b*, 2+ (benign); *c*, 3+ (malignant); *d*, 4+ (malignant).

We assessed whether there was any correlation between the level of IGF1R staining and serum PSA or Gleason grade. There was a trend toward higher PSA values in patients with tumors staining 3+ to 4+ for IGF1R, reflecting the predominance of malignant prostate biopsies in this group. However, there was a wide range of PSA values in each staining group, and statistical analysis showed no significant difference between mean PSA values in tumors staining 1+ to 4+ for IGF1R. Similarly, there was no evidence that the IGF1R staining intensity was related to Gleason grade in the prostate cancer biopsies. However within the individual areas used for scoring, the major component had Gleason grades of 3 or 4; this point could be clarified by performing IGF1R immunohistochemistry on malignant biopsies spanning a wider range of Gleason grades.

To verify that the IGF1R antibody did not cross-react with other tissue antigens, fresh prostate tissue lysates were analyzed by immunoblotting with the same IGF1R $\beta$  antibody used for immunohisto-

chemistry. This confirmed that the antibody was indeed detecting the  $M_r$  98,000 IGF1R  $\beta$ -subunit, without significant cross-reaction with other proteins. There was a trend toward higher IGF1R levels in the cancer lysates than in the benign samples (not shown). However, these samples had not been microdissected, and this result could be influenced by benign epithelium and stromal elements contaminating the carcinoma biopsies.

To compare IGF1R expression at the protein and RNA levels we performed *in situ* hybridization on prostate biopsy tissue. Initial evaluation of sections of fine-needle biopsies indicated poor hybridization to the  $\beta$ -actin probe, perhaps because of overfixation (not shown). Therefore, we used uniformly fixed, prospectively collected biopsies for *in situ* hybridization. Immunohistochemical analysis of adjacent sections showed that IGF1R expression in these prospectively collected specimens followed the pattern seen in the archival fine-needle biopsies described above. All of the benign biopsies stained either nil or light (1+ to 2+), and the IGF1R staining in the malignant tissue was light, moderate, or heavy (2+ to 4+). *In situ* hybridization analysis of these prospectively collected biopsies revealed detectable and appropriate hybridization to the  $\beta$ -actin probe, with strong labeling of vascular smooth muscle cells and lymphocyte aggregates, and variable labeling of other cell types (Fig. 5, *a* and *e*). The sense IGF1R probe did not hybridize to any tissue sections (not shown). The antisense IGF1R probe gave weak-to-moderate signal over areas of benign epithelium (Fig. 5, *b–d*). More intense hybridization was seen in areas of malignant epithelium that corresponded to areas of increased IGF1R protein detected by immunohistochemistry (Fig. 5, *f–h*). These results are consistent with the regulation of IGF1R expression at the transcriptional level.

**IRS-1 Is Expressed by Benign and Malignant Prostatic Epithelium.** To check the specificity of IRS-1 immunostaining, we prepared cell pellets from human prostate cancer cell lines DU145 and LNCaP.

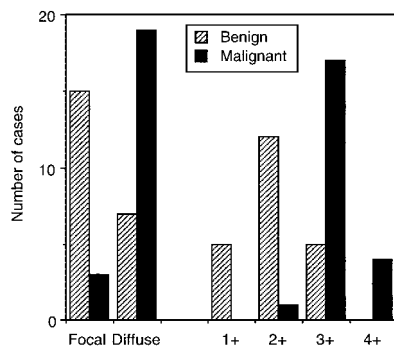


Fig. 4. Analysis of immunohistochemical IGF1R staining of primary prostate cancer. The pattern of staining was recorded as focal or diffuse. The staining intensity was scored using a 4-point scale: 1+, none or minimal; 2+, light; 3+, moderate; 4+, heavy, as described previously (13).

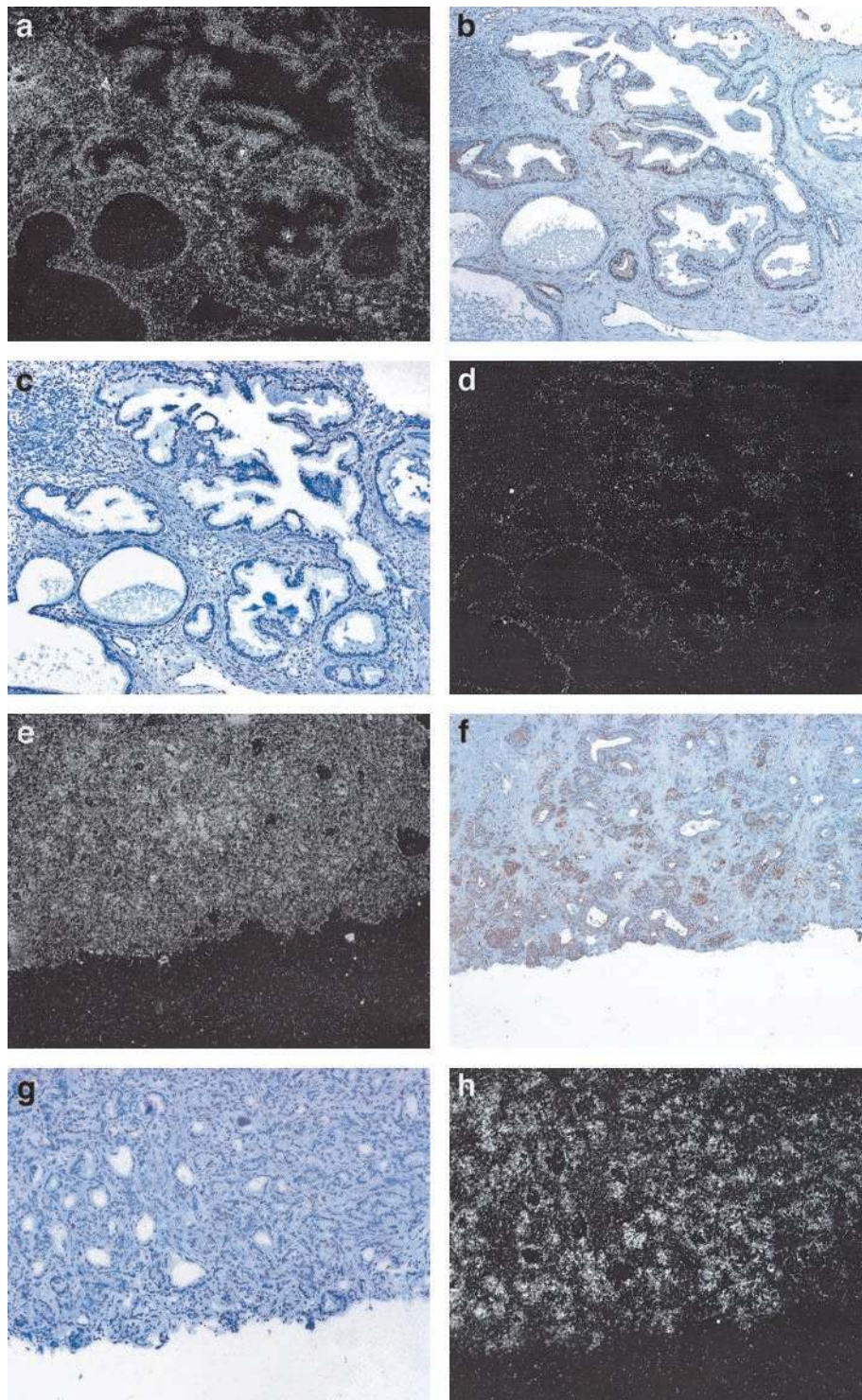


Fig. 5. Analysis of IGF1R expression by *in situ* hybridization. *a–d*, sections of a benign biopsy; *e–h*, sections of a prostate adenocarcinoma. *a* and *e*, hybridization to  $\beta$ -actin probe (8-day exposure); *b* and *f*, immunohistochemical analysis of IGF1R protein expression; *c* and *g*, bright-field illumination; *d* and *h*, dark-field illumination, showing hybridization to antisense IGF1R probe (8-day exposure).  $\times 100$ .

Both of these cell types express the IGF1R, detectable by immunoblotting and immunostaining (not shown). DU145 cells also express IRS-1, but LNCaP cells reportedly lack IRS-1 because of promoter methylation (9). Indeed, we were unable to detect IRS-1 by immunostaining of LNCaP cells, whereas DU145 cells showed clear membranous and cytoplasmic staining (Fig. 1, *c* and *d*). Immunoblotting with the same IRS-1 antibody revealed a single band of  $M_r \sim 180,000$  in DU145 cells, and no band in LNCaP cells (not shown).

IRS-1 expression was assessed in a subset of the fine-needle biopsies used for analysis of IGF1R immunostaining, including 11

sections of malignant prostate that had the highest expression of IGF1R (3+ or 4+) and the 11 sections of benign prostate that had the lowest IGF1R levels (1+ or 2+). We also assessed IRS-1 expression in the 10 prostate biopsy chips that we had prospectively collected for analysis of IGF1R expression by *in situ* hybridization. Fig. 6 shows representative sections of benign and malignant prostate biopsies stained for IGF1R and IRS-1. The results for all specimens are shown in Table 1, including the 22 retrospectively collected and 10 prospectively collected biopsies. In both the benign and malignant prostate biopsies there was a

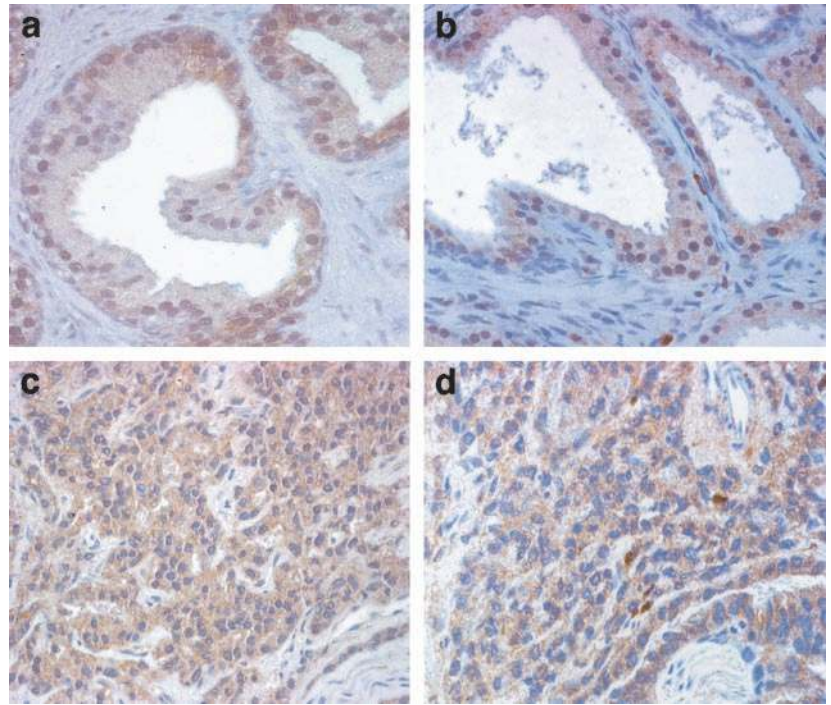


Fig. 6. Semiquantitative immunostaining for IGF1R and IRS-1 in fine-needle biopsies of the prostate. Comparison of benign (a and b) and malignant (c and d) prostate biopsies for IGF1R (a and c) and for IRS-1 (b and d) staining ( $\times 200$ ). IRS-1 shows positive staining in the cytoplasm of epithelial cells, with strong staining in stromal macrophages.

trend toward higher IRS-1 staining in biopsies with high IGF1R levels. However, the difference in intensity of IRS-1 staining between benign and malignant epithelium was less marked than was the difference in IGF1R staining, and failed to reach statistical significance.

**IGF1R and IRS-1 Are Infrequently Down-Regulated in Metastatic Prostate Cancer.** To assess any changes in IGF1R and IRS-1 expression in metastatic prostate cancer, we analyzed IGF1R and IRS-1 levels by immunostaining in 12 cases, in which we were able to obtain paired biopsies of primary and metastatic tumor (Table 2). The interval between the diagnostic and metastatic biopsies was 5–108 months (median, 19.5 months). In 4 patients with early relapse (5–8 months after initial biopsy), the prostate tumor showed evidence of high grade-disease with neurovascular invasion (cases 3, 5, 9, and 11 in Table 2). There were 6 cases (1–6 in Table 2) in which IGF1R levels were unchanged or higher in the metastasis compared with the primary tumor. In the other six, IGF1R levels appeared to be lower in the metastatic deposit than in the primary. In two of these (cases 7, 8) the reduction was from 4+ to 3+ intensity, indicating persistence of significant IGF1R expression in the metastasis. Fig. 7(a, d) shows representative sections from case 7. In the remaining 4 cases (9–12 in Table 2), IGF1R levels fell from 2+–4+ in the primary tumors to 1+–2+ in the metastases (Fig. 7g, j). Table 2 also shows the results of

semiquantitative analysis of IRS-1 expression in these paired tumor biopsies. As before the levels of IRS-1 staining tended to parallel the intensity of IGF1R staining. There were 4 cases (nos. 1, 10, 11, 12) where IRS-1 expression fell to 1+ (nil/negligible) in the metastatic deposit (Fig. 7 h, k); all other cases retained significant ( $\geq 2+$ ) IRS-1 expression (Fig. 7b, e). Therefore our results show significant retention and in some cases up-regulation of IGF1R and IRS-1 in metastatic deposits of prostate cancer.

**Down-Regulation of IGF1R and IRS-1 Can Be Associated with Loss of PTEN Expression.** Finally we assessed the presence of PTEN immunoreactivity. Initially we stained sections made from cell pellets of the DU145 cell line (one wild type PTEN allele), and the PC-3 cell line (homozygous PTEN gene deletion), which were previously identified as appropriate positive and negative controls respectively (27, 28, 39). Indeed the DU145 cells showed definite granular cytoplasmic staining for PTEN, whereas PC-3 cells showed no detectable staining (Fig. 1e, f). Immunohistochemical staining of primary prostate biopsies revealed that PTEN was undetectable in two primary tumors (17%, cases 1 and 3 in Table 2), although it was detected in the metastasis from case 3. The remaining 10 primary tumors had detectable PTEN staining that was of uniform intensity but variable extent (Fig. 7c, i). Three cases (25%) showed mixed staining (1+ in Table 2), with some tumor cells positive and some negative for PTEN. In 7 cases (58%) all of the tumor cells were positive (2+) for immunoreactive PTEN. This compares with a previous report of 109 cases of primary prostate cancer in which PTEN staining was negative in 20%, mixed in 65% and positive in 15% (28). The complete absence of PTEN correlated significantly with a Gleason score of  $\geq 7$ , and with advanced (T3b and T4) stage (28). In our series the two primary tumors which lacked PTEN had total Gleason scores of 6 (case 1) and 7 (case 3). In most of the cases where PTEN was present in the primary, we were able to detect PTEN in the metastasis at similar or increased levels (Fig. 7f). However there were three tumors that had apparently lost PTEN expression during the progression to androgen-independent metastatic disease (Fig. 7l, cases 10–12 in Table 2). It was notable that all three of these cases had shown

Table 1 Semiquantitative analysis of IRS-1 expression in prostate biopsies

The staining intensity was scored as for IGF1R expression using a 4-point scale: 1+, none or minimal; 2+, light; 3+, moderate; 4+, heavy. The Table records staining for 16 benign (B) and 16 malignant (M) biopsies, including 11 benign and 11 malignant retrospectively collected fine-needle biopsies used for IGF1R analysis, and 5 benign, 5 malignant prospectively-collected samples.

IGF1R	IRS-1							
	1+		2+		3+		4+	
	B	M	B	M	B	M	B	M
1+	1	0	6	0	3	0	0	0
2+	0	0	1	0	4	2	1	0
3+	0	0	0	2	0	3	0	4
4+	0	0	0	0	0	4	0	1

Table 2 Immunohistochemical staining for IGF1R, IRS-1, and PTEN in paired biopsies of primary and metastatic prostate cancer

Table shows staining intensity (IGF1R and IRS-1) and extent (PTEN) in paired primary (P) and metastatic (M) human prostate cancer tissue. For IGF1R and IRS-1, staining intensity was scored as for Fig. 3 and Table 1. The extent of PTEN staining was scored as 0 (no staining), 1+ (mixed, some tumor cells positive, some negative) or 2+ (all tumor cells positive), as described previously (28).

Case	Total Gleason Score	IGF1R		IRS-1		PTEN	
		P	M	P	M	P	M
1	6	3	3	2	1	0	0
2	6	1	2	3	2	1	2
3	7	2	4	2	3	0	2
4	9	1	4	3	4	2	2
5	8	2	2	2	2	2	2
6	6	1	4	1	4	2	2
7	8	4	3	4	4	2	2
8	6	4	3	4	4	2	2
9	9	4	2	3	2	1	1
10	7	2	1	3	1	2	0
11	8	3	1	4	1	2	0
12	7	2	1	3	1	1	0

significant reduction in both IGF1R and IRS-1 expression in the metastasis compared with the primary biopsy.

## DISCUSSION

We used a previously validated semiquantitative immunohistochemical method (13) to show that there is diffuse increased expression of the IGF1R in localized human prostate cancer. This result conflicts with previous reports using immunostaining and immunoblotting to quantify IGF1R levels in prostate cancer (18, 20). It may be difficult to interpret results of analysis of IGF1R levels by the immunoblotting of tissue lysates, because of contaminating stromal elements and benign epithelium in the malignant biopsies. In a few samples, we found a trend toward higher IGF1R levels in lysates made from malignant biopsies, but the magnitude of the difference between benign and malignant epithelia was less marked than was apparent by immunostaining.

It seems likely that technical factors could explain why our results differ from those of previous studies. We undertook preliminary optimization of immunostaining, which proved important in obtaining reliable staining results for IGF1R and PTEN. The intensity of staining can be affected by the size of biopsy and hence the adequacy of formalin-fixation, which has an important influence on the rate of decay of immunoreactivity (34). The outcome can also be influenced by the choice of "normal" tissue controls, the use of antigen-retrieval techniques, and by the type and amount of antibody used for staining. We found that the use of the IGF1R $\beta$  antibody at a higher concentration than 1:750 was sufficient to abolish apparent differences in IGF1R staining between benign and malignant prostate epithelium (not shown). The results can also be influenced by the choice of secondary reagents used to detect bound primary antibody. We used the Envision system, which is more sensitive than the standard ABC kit (Ref. 40 and our unpublished observations). We used the appropriate cell controls to guide our choice of antibody dilution for staining studies and incorpo-

rated positive and negative controls into each staining run. These factors may explain the discrepancies between our findings and those of previous reports (18, 19).

The results of immunohistochemical analysis were reinforced by *in situ* hybridization, which showed that the increase in IGF1R expression in prostate cancer was attributable to enhanced expression at the level of gene transcription. This result concurs with that of Kurek *et al.* (41), who used quantitative reverse transcription-PCR to show a 10-fold up-regulation of IGF1R expression in primary prostate cancer *versus* benign prostatic epithelium. A trend to IGF1R up-regulation in prostate cancer was also reported by Figueroa *et al.* (42). The finding of IGF1R overexpression has been reported in other tumor types (10, 11), and also tallies with the ability to inhibit prostate cancer growth by blocking expression or function of the IGF1R (31, 43). However, IGF1R up-regulation has not been reported in recent studies using gene arrays to profile prostate cancer (44–47). In one of these studies, the on-line supplementary material indicated that IGF1R levels were similar in the primary cancers to the control samples of normal prostate. However, IGF1R levels in the BPH samples were generally lower than in the normal samples, which illustrates the influence of the selection of nonmalignant control tissues. Compared with BPH, there was an apparent increase in IGF1R expression of ~25% in primary prostate cancer and ~50% in metastatic disease (44). Furthermore, differential expression of IGF-II and IGF BP2 and -BP5 was observed in prostate cancer (44, 47) and differential expression of IGF BP4 was observed in prostatic intraepithelial neoplasia (45), supporting the importance of this growth factor pathway.

There is little information on IGF1R expression in advanced prostate cancer. One study reported that the IGF1R was undetectable in bone metastases (19), and IGF1R levels have been reported to fall in lymph node metastases in the TRAMP model (22). It should be noted, however, that SV40 immortalization has itself been shown to influence cellular IGF-I and IGF1R levels (48, 49). This model does not recapitulate all of the cellular and molecular changes involved in prostate cancer pathogenesis. Indeed, transgenic rats, expressing SV40 T antigen driven by the probasin promoter, develop prostate carcinomas that are strictly androgen dependent (50). These studies have, however, led to a consensus view that IGF1R levels are down-regulated in metastatic disease (4, 24, 51). As outlined above, Dr. Baserga's group has proposed that IRS-1 loss might favor metastasis, in which case, IGF1R down-regulation is necessary to avoid Shc-mediated terminal differentiation (4, 9, 52). In this setting, activation of the phosphatidylinositol triphosphate pathway is achieved by *PTEN* mutation (27).

Our analysis of paired primary and metastatic prostate cancer biopsies revealed some cases in which the IGF1R was down-regulated in metastatic disease, compatible with findings in the TRAMP model (22). This was associated with down-regulation of IRS-1 and with significant reduction/loss of PTEN immunostaining. This pattern was relatively uncommon, occurring in 3 of 12 cases that we analyzed. Thus, our study provides limited support for the relevance of the cellular and molecular changes occurring in model systems of prostate cancer. However, most of the tumors that we studied continued to express IGF1R and IRS-1 during the development of advanced, androgen-independent metastatic disease. In support of this finding, Nickerson *et al.* (53) have reported significant up-regulation of both IGF-I and the IGF1R during progression to androgen-independent growth of LNCaP and LAPC-9 tumors *in vivo*. These findings confirm that the IGF axis plays an important role in prostate cancer biology and

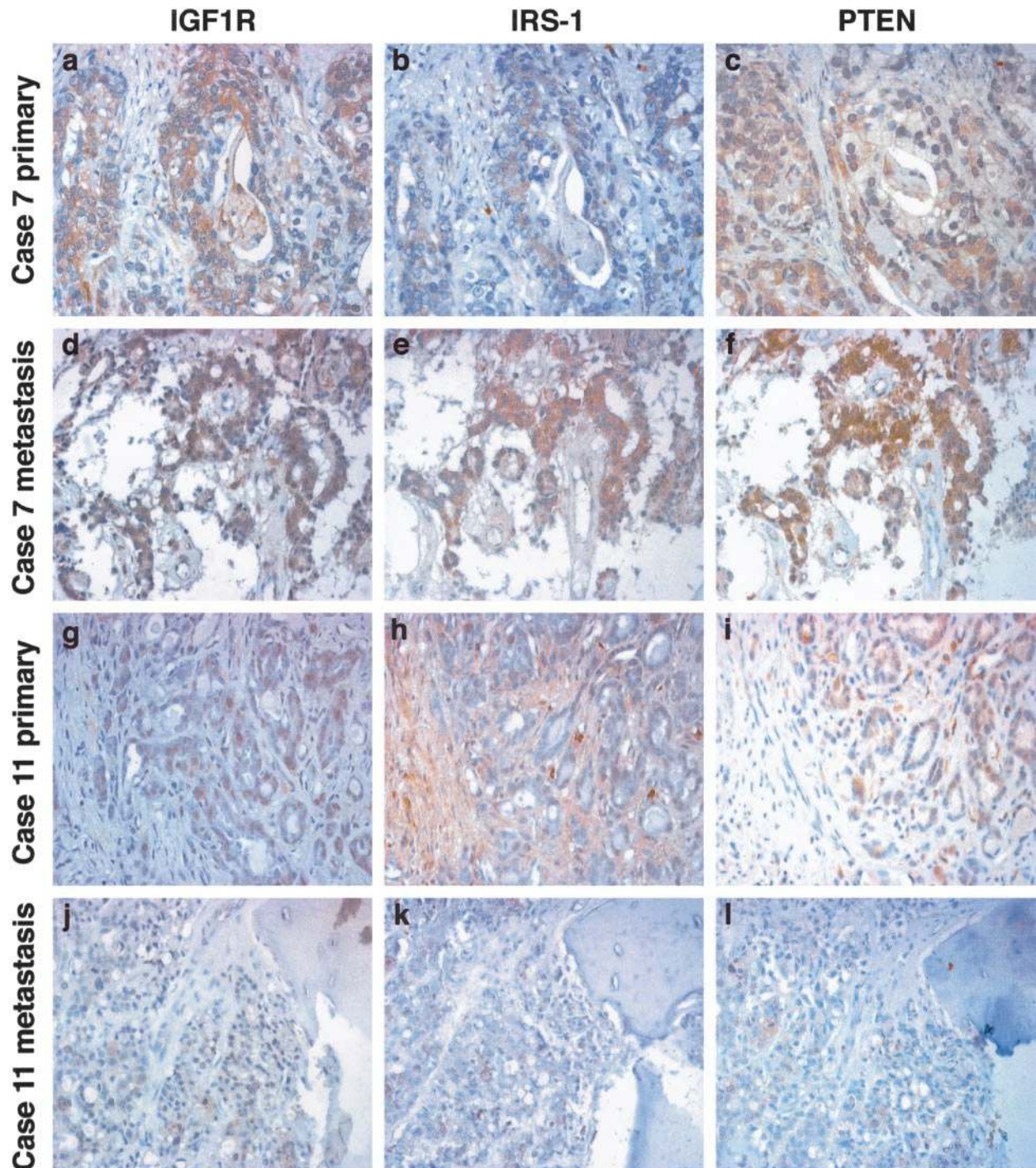


Fig. 7. Immunohistochemical staining for IGF1R, IRS-1, and PTEN in paired biopsies of primary and metastatic prostate cancer. *a–c*, sections from the primary tumor of case 7, showing expression of IGF1R (*a*), IRS-1 (*b*), and PTEN (*c*) in the primary biopsy; *d–f*, sections from the metastasis of case 7 (Table 2), showing the persistence of expression of IGF1R (*d*), IRS-1 (*e*), and PTEN (*f*) in the secondary deposit ( $\times 200$ ). *g–i*, from the primary tumor; *j–l*, from the metastasis of case 11. The primary tumor expressed IGF1R (*g*), IRS-1 (*h*) and PTEN (*i*) but immunoreactive IGF1R (*j*), IRS-1 (*k*) and PTEN (*l*) were significantly reduced in the metastasis.  $\times 100$ .

support the concept of IGF1R targeting as a potential treatment for metastatic prostate cancer.

#### ACKNOWLEDGMENTS

We are grateful to Renato Baserga, Kimmel Cancer Center, Thomas Jefferson University, Philadelphia, PA, for cell lines, IGF1R cDNA, and advice; and to Dr. Athanasou, Department of Pathology, Nuffield Orthopaedic Centre, Oxford, United Kingdom, for help in obtaining paired tumor biopsies. For technical help, we thank Rosemary Jeffery and Jan Longcroft of the Cancer

Research UK *In Situ* Hybridisation Service, and Robin Roberts-Gant, Medical Informatics Unit, Nuffield Department of Clinical Laboratory Sciences, John Radcliffe Hospital, Oxford, United Kingdom.

#### REFERENCES

1. Parker, S. L., Tong, T., Bolden, S., and Wingo, P. A. Cancer statistics, 1997. *CA Cancer J. Clin.*, 47: 5–27, 1997.
2. Byrne, R. L., Leung, H., and Neal, D. E. Peptide growth factors in the prostate as mediators of stromal epithelial interaction. *Br. J. Urol.*, 77: 627–633, 1996.
3. Brewster, S. F., and Gillatt, D. A. Advanced prostate cancer: what's new in hormonal manipulation? *Br. J. Hosp. Med.*, 49: 710–711, 714–715, 1993.



4. Baserga, R. The IGF-I receptor in cancer research. *Exp. Cell Res.*, *253*: 1–6, 1999.
5. Jackson, J. G., Zhang, X., Yoneda, T., and Yee, D. Regulation of breast cancer cell motility by insulin receptor substrate-2 (IRS-2) in metastatic variants of human breast cancer cell lines. *Oncogene*, *20*: 7318–7325, 2001.
6. Maile, L. A., Imai, Y., Badley Clarke, J., and Clemmons, D. R. Insulin-like growth factor-1 increases  $\alpha V\beta 3$  affinity by increasing the amount of integrin-associated protein that is associated with non raft domains of the cellular membrane. *J. Biol. Chem.*, *277*: 1800–1805, 2001.
7. Playford, M. P., Bicknell, D., Bodmer, W. F., and Macaulay, V. M. Insulin-like growth factor 1 regulates the location, stability, and transcriptional activity of  $\beta$ -catenin. *Proc. Natl. Acad. Sci. USA*, *97*: 12103–12108, 2000.
8. Guvakova, M. A., and Surmacz, E. Overexpressed IGF-I receptors reduce estrogen growth requirements, enhance survival, and promote E-cadherin-mediated cell-cell adhesion in human breast cancer cells. *Exp. Cell Res.*, *231*: 149–162, 1997.
9. Reiss, K., Wang, J. Y., Romano, G., Furnari, F. B., Cavenee, W. K., Morrione, A., Tu, X., and Baserga, R. IGF-I receptor signaling in a prostatic cancer cell line with a PTEN mutation. *Oncogene*, *19*: 2687–2694, 2000.
10. Hakam, A., Yeatman, T. J., Lu, L., Mora, L., Marcet, G., Nicosia, S. V., Karl, R. C., and Coppola, D. Expression of insulin-like growth factor-1 receptor in human colorectal cancer. *Hum. Pathol.*, *30*: 1128–1133, 1999.
11. Kanter-Lewensohn, L., Dricu, A., Girmata, L., Wejde, J., and Larsson, O. Expression of insulin-like growth factor-1 receptor (IGF-1R) and p27Kip1 in melanocytic tumors: a potential regulatory role of IGF-1 pathway in distribution of p27Kip1 between different cyclins. *Growth Factors*, *17*: 193–202, 2000.
12. Khandwala, H. M., McCutcheon, I. E., Flyvbjerg, A., and Friend, K. E. The effects of insulin-like growth factors on tumorigenesis and neoplastic growth. *Endocr. Rev.*, *21*: 215–244, 2000.
13. Turner, B. C., Haffey, B. G., Narayanan, L., Yuan, J., Havre, P. A., Gumbs, A. A., Kaplan, L., Burgaud, J. L., Carter, D., Baserga, R., and Glazer, P. M. Insulin-like growth factor-1 receptor overexpression mediates cellular radioresistance and local breast cancer recurrence after lumpectomy and radiation. *Cancer Res.*, *57*: 3079–3083, 1997.
14. Macaulay, V. M., Salisbury, A. J., Bohula, E. A., Playford, M. P., Smorodinsky, N. I., and Shiloh, Y. Downregulation of the type I insulin-like growth factor receptor in mouse melanoma cells is associated with enhanced radiosensitivity and impaired activation of Atm kinase. *Oncogene*, *20*: 4029–4040, 2001.
15. Chan, J. M., Stampfer, M. J., Giovannucci, E., Gann, P. H., Ma, J., Wilkinson, P., Hennekens, C. H., and Pollak, M. Plasma insulin-like growth factor-I and prostate cancer risk: a prospective study. *Science (Wash. DC)*, *279*: 563–566, 1998.
16. Wolk, A., Mantzoros, C. S., Andersson, S. O., Bergstrom, R., Signorello, L. B., Lagiou, P., Adami, H. O., and Trichopoulos, D. Insulin-like growth factor I and prostate cancer risk: a population-based, case-control study. *J. Natl. Cancer Inst. (Bethesda)*, *90*: 911–915, 1998.
17. Cohen, P., Peehl, D. M., Lamson, G., and Rosenfeld, R. G. Insulin-like growth factors (IGFs), IGF receptors, and IGF-binding proteins in primary cultures of prostate epithelial cells. *J. Clin. Endocrinol. Metab.*, *73*: 401–407, 1991.
18. Tennant, M. K., Thrasher, J. B., Twomey, P. A., Drivdahl, R. H., Birnbaum, R. S., and Plymate, S. R. Protein and messenger ribonucleic acid (mRNA) for the type I insulin-like growth factor (IGF) receptor is decreased and IGF-II mRNA is increased in human prostate carcinoma compared to benign prostate epithelium. *J. Clin. Endocrinol. Metab.*, *81*: 3774–3782, 1996.
19. Chott, A., Sun, Z., Morganstern, D., Pan, J., Li, T., Susani, M., Mosberger, I., Upton, M. P., Buble, G. J., and Balk, S. P. Tyrosine kinases expressed *in vivo* by human prostate cancer bone marrow metastases and loss of the type I insulin-like growth factor receptor. *Am. J. Pathol.*, *155*: 1271–1279, 1999.
20. Zhang, P., Wang-Rodriguez, J., and Bailey, D. Insulin-like growth factor receptor expression in prostate cancer. *Am. J. Clin. Pathol.*, *112*: 130, 1999.
21. Gingrich, J. R., Barrios, R. J., Morton, R. A., Boyce, B. F., DeMayo, F. J., Finegold, M. J., Angelopoulos, R., Rosen, J. M., and Greenberg, N. M. Metastatic prostate cancer in a transgenic mouse. *Cancer Res.*, *56*: 4096–4102, 1996.
22. Kaplan, P. J., Mohan, S., Cohen, P., Foster, B. A., and Greenberg, N. M. The insulin-like growth factor axis and prostate cancer: lessons from the transgenic adenocarcinoma of mouse prostate (TRAMP) model. *Cancer Res.*, *59*: 2203–2209, 1999.
23. Horoszewicz, J. S., Leong, S. S., Chu, T. M., Wajzman, Z. L., Friedman, M., Papsidero, L., Kim, U., Chai, L. S., Kakati, S., Arya, S. K., and Sandberg, A. A. The LNCaP cell line—a new model for studies on human prostatic carcinoma. *Prog. Clin. Biol. Res.*, *37*: 115–132, 1980.
24. Baserga, R. The contradictions of the insulin-like growth factor I receptor. *Oncogene*, *19*: 5574–5581, 2000.
25. Reiss, K., D'Ambrosio, C., Tu, X., Tu, C., and Baserga, R. Inhibition of tumor growth by a dominant negative mutant of the insulin-like growth factor I receptor with a bystander effect. *Clin. Cancer Res.*, *4*: 2647–2655, 1998.
26. Baserga, R., Hongo, A., Rubini, M., Prisco, M., and Valentini, B. The IGF-I receptor in cell-growth, transformation and apoptosis. *Biochim. Biophys. Acta*, *1332*: F105–F126, 1997.
27. Li, J., Yen, C., Liaw, D., Podsypanina, K., Bose, S., Wang, S. I., Puc, J., Miliareis, C., Rodgers, L., McCombie, R., Bigner, S. H., Giovannella, B. C., Irtmann, M., Tycko, B., Hibshoosh, H., Wigler, M. H., and Parsons, R. *PTEN*, a putative protein tyrosine phosphatase gene mutated in human brain, breast, and prostate cancer. *Science (Wash. DC)*, *275*: 1943–1947, 1997.
28. McMenamin, M. E., Soung, P., Perera, S., Kaplan, I., Loda, M., and Sellers, W. R. Loss of PTEN expression in paraffin-embedded primary prostate cancer correlates with high Gleason score and advanced stage. *Cancer Res.*, *59*: 4291–4296, 1999.
29. Davies, M. A., Koul, D., Dhesi, H., Berman, R., McDonnell, T. J., McConkey, D., Yung, W. K., and Steck, P. A. Regulation of Akt/PKB activity, cellular growth, and apoptosis in prostate carcinoma cells by MMAC/PTEN. *Cancer Res.*, *59*: 2551–2556, 1999.
30. Iwamura, M., Sluss, P. M., Casamento, J. B., and Cockett, A. T. Insulin-like growth factor I: action and receptor characterization in human prostate cancer cell lines. *Prostate*, *22*: 243–252, 1993.
31. Pietrzakowski, Z., Mulholland, G., Gomella, L., Jameson, B. A., Wernicke, D., and Baserga, R. Inhibition of growth of prostatic cancer cell lines by peptide analogues of insulin-like growth factor I. *Cancer Res.*, *53*: 1102–1106, 1993.
32. Kimura, G., Kasuya, J., Giannini, S., Honda, Y., Mohan, S., Kawachi, M., Akimoto, M., and Fujita-Yamaguchi, Y. Insulin-like growth factor (IGF) system components in human prostatic cancer cell-lines: LNCaP, DU145, and PC-3 cells. *Int. J. Urol.*, *3*: 39–46, 1996.
33. Sell, C., Dumenil, G., Deveaud, C., Miura, M., Coppola, D., Deangelis, T., Rubin, R., Efstratiadis, A., and Baserga, R. Effect of a null mutation of the *insulin-like growth-factor-1 receptor* gene on growth and transformation of mouse embryo fibroblasts. *Mol. Cell. Biol.*, *14*: 3604–3612, 1994.
34. Vis, A. N., Kranse, R., Nigg, A. L., and van der Kwast, T. H. Quantitative analysis of the decay of immunoreactivity in stored prostate needle biopsy sections. *Am. J. Clin. Pathol.*, *113*: 369–373, 2000.
35. Ramaswamy, S., Nakamura, N., Vazquez, F., Batt, D. B., Perera, S., Roberts, T. M., and Sellers, W. R. Regulation of G<sub>1</sub> progression by the PTEN tumor suppressor protein is linked to inhibition of the phosphatidylinositol 3-kinase/Akt pathway. *Proc. Natl. Acad. Sci. USA*, *96*: 2110–2115, 1999.
36. Senior, P. V., Critchley, D. R., Beck, F., Walker, R. A., and Varley, J. M. The localization of laminin mRNA and protein in the postimplantation embryo and placenta of the mouse: an *in situ* hybridization and immunocytochemical study. *Development (Camb.)*, *104*: 431–446, 1988.
37. Ullrich, A., Gray, A., Tam, A. W., Yang-Feng, T., Tsubokawa, M., Collins, C., Henzel, W., Le Bon, T., Kathuria, S., Chen, E. *et al.* Insulin-like growth factor I receptor primary structure: comparison with insulin receptor suggests structural determinants that define functional specificity. *EMBO J.*, *5*: 2503–2512, 1986.
38. Zandvliet, D. W., Hanby, A. M., Austin, C. A., Marsh, K. L., Clark, I. B., Wright, N. A., and Poulos, R. Analysis of foetal expression sites of human type II DNA topoisomerase  $\alpha$  and  $\beta$  mRNAs by *in situ* hybridisation. *Biochim. Biophys. Acta*, *1307*: 239–247, 1996.
39. Taniyama, K., Goodison, S., Ito, R., Bookstein, R., Miyoshi, N., Tahara, E., Tarin, D., and Urquidí, V. PTEN expression is maintained in sporadic colorectal tumours. *J. Pathol.*, *194*: 341–348, 2001.
40. Sabattini, E., Bisgaard, K., Ascani, S., Poggi, S., Piccioli, M., Ceccarelli, C., Pieri, F., Fraternali-Orcioni, G., and Pileri, S. A. The EnVision++ system: a new immunohistochemical method for diagnostics and research. Critical comparison with the APAAP, ChemMate, CSA, LABC, and SABC techniques. *J. Clin. Pathol.*, *51*: 506–511, 1998.
41. Kurek, R., Tunn, U. W., Ammueller, G., and Renneberg, H. Insulin-like growth factor-1 (IGF-1) and insulin-like growth factor receptor (IGF-R1) in prostate cancer. *J. Urol.*, *163* (Suppl.): 35, 2000.
42. Figueroa, J. A., De Raad, S., Speights, V. O., and Rinehart, J. J. Gene expression of insulin-like growth factors and receptors in neoplastic prostate tissues: correlation with clinico-pathological parameters. *Cancer Investig.*, *19*: 28–34, 2001.
43. Burfeind, P., Chermicky, C. L., Rininsland, F., and Ilan, J. Antisense RNA to the type I insulin-like growth factor receptor suppresses tumor growth and prevents invasion by rat prostate cancer cells *in vivo*. *Proc. Natl. Acad. Sci. USA*, *93*: 7263–7268, 1996.
44. Dhanasekaran, S. M., Barrette, T. R., Ghosh, D., Shah, R., Varambally, S., Kurachi, K., Pienta, K. J., Rubin, M. A., and Chinnaiyan, A. M. Delineation of prognostic biomarkers in prostate cancer. *Nature (Lond.)*, *412*: 822–826, 2001.
45. Bull, J. H., Ellison, G., Patel, A., Muir, G., Walker, M., Underwood, M., Khan, F., and Paskins, L. Identification of potential diagnostic markers of prostate cancer and prostatic intraepithelial neoplasia using cDNA microarray. *Br. J. Cancer*, *84*: 1512–1519, 2001.
46. Chcutici, A., Margan, S., Mann, S., Russell, P., Handelsman, D., Rogers, J., and Dong, Q. Identification of differentially expressed genes in organ-confined prostate cancer by gene expression array. *Prostate*, *47*: 132–140, 2001.
47. Chaib, H., Cockrell, E. K., Rubin, M. A., and Macoska, J. A. Profiling and verification of gene expression patterns in normal and malignant human prostate tissues by cDNA microarray analysis. *Neoplasia*, *3*: 43–52, 2001.
48. Porcu, P., Ferber, A., Pietrzakowski, Z., Roberts, C. T., Adamo, M., LeRoith, D., and Baserga, R. The growth-stimulatory effect of simian virus 40 T antigen requires the interaction of insulinlike growth factor I with its receptor. *Mol. Cell. Biol.*, *12*: 5069–5077, 1992.
49. Zilberstein, M., Chou, J. Y., Lowe, W. L., Jr., Shen-Orr, Z., Roberts, C. T., Jr., LeRoith, D., and Catt, K. J. Expression of insulin-like growth factor-I and its receptor by SV40-transformed rat granulosa cells. *Mol. Endocrinol.*, *3*: 1488–1497, 1989.
50. Asamoto, M., Hokiawado, N., Cho, Y. M., Takahashi, S., Ikeda, Y., Imaida, K., and Shirai, T. Prostate carcinomas developing in transgenic rats with SV40 T antigen expression under probasin promoter control are strictly androgen dependent. *Cancer Res.*, *61*: 4693–4700, 2001.
51. Plymate, S. R., Bae, V. L., Maddison, L., Quinn, L. S., and Ware, J. L. Reexpression of the type-I insulin-like growth-factor receptor inhibits the malignant phenotype of simian-virus-40 t-antigen immortalized human prostate epithelial-cells. *Endocrinology*, *138*: 1728–1735, 1997.
52. Reiss, K., Wang, J. Y., Romano, G., Tu, X., Peruzzi, F., and Baserga, R. Mechanisms of regulation of cell adhesion and motility by insulin receptor substrate-1 in prostate cancer cells. *Oncogene*, *20*: 490–500, 2001.
53. Nickerson, T., Chang, F., Lorimer, D., Smeekens, S. P., Sawyers, C. L., and Pollak, M. *In vivo* progression of LAPC-9 and LNCaP prostate cancer models to androgen independence is associated with increased expression of insulin-like growth factor I (IGF-I) and IGF-I receptor (IGF-IR). *Cancer Res.*, *61*: 6276–6280, 2001.